Journal of Statistical Physics, Vol. 94, Nos. 1/2, 1999

Analytical and Numerical Studies of the One-Dimensional Spin Facilitated Kinetic Ising Model

Michael Schulz[1] and Steffen Trimper[1]

Received February 8, 1998; final September 10, 1998

The one-dimensional spin facilitated kinetic Ising model is studied analytically using the master equation and by simulations. The local state of the spins (corresponding to mobile and immobile cells) can change depending on the state of the neighbored spins, which reflects the high cooperativity inherent in glassy materials. The short-time behavior is analyzed using a Fock space representation for the master equation. The hierarchy of evolution equations for the averaged spin state and the time dependence of the spin autocorrelation function are calculated with different methods (mean-field theory, expansion in powers of the time, partial summation) and compared with numerical simulations. The long-time behavior can be obtained by mapping the one-dimensional spin facilitated kinetic Ising model onto a one-dimensional diffusion model containing birth and death processes. The resulting master equation is solved by van Kampen's size expansion, which leads to a Langevin equation with Gaussian noise. The predicted autocorrelation function and the global memory offer in the long-time limit a screened algebraic decay and a stretched exponential decay, respectively, consistent with numerical simulations.

KEY WORDS: Lattice theory; nonequilibrium kinetics; glass transition.

I. INTRODUCTION

In spite of advances in the description of liquids near the glass transition using different approaches[1–4] the phenomenon is generally not complete understooden. Supercooled fluids reveal often a non-Arrhenius behavior of the relaxation spectrum such as it is manifested in a stretched exponential decay of the correlation function. In contrast to conventional phase transitions a long range order is not developed. However, the dynamical glass

[1] Fachbereich Physik, Martin-Luther-Universität, 06099 Halle, Germany.

0022-4715/99/0100-0173$16.00/0

transition can be described by an increasing cooperativity of local processes with decreasing temperature.[5] The cooperativity leads to the well known slowing down in the dynamical behavior (non-Arrhenius) which can be illustrated by a strongly curved trajectory in the Arrhenius plot (relaxation time τ versus the inverse temperature T^{-1}). One possible fit of this curve is given by the Williams–Landel–Ferry (WLF) curve[6] with $\ln \tau \propto (T - T_0)^{-1}$ and a finite Vogel temperature T_0. The α-process is an universal phenomena of the glass transition. There is a general suggestion that the α-process corresponds mainly to the cooperative molecular diffusion, e.g., the diffusion coefficient D and the α relaxation time τ_α are often related by $D\tau_\alpha \simeq 1$.

Mode coupling theories[1, 7, 8] (MCT) predict the existence of an ergodic α-process above a kinetic critical temperature T_c and a nonergodic β-process below T_c. Note that T_c is in the range between the melting temperature T_m and the glass temperature T_g, e.g., $T_m > T_c > T_g$. At T_c the system undergoes a sharp phase transition to a state with frozen (density) fluctuations. The α-process within the MCT is thought to correspond to the actual dynamic glass transition whereas the β-process is often identified with a cage rattling or the boson peak.

Really the α process still exists below T_c. This process leads to a slow decay of apparently frozen structures (The nonergodic structures obtained from the MCT are approximately stable only for a finite time interval). This slow decay shows the typical properties which correspond usually to the dynamics of the main glass transition (WLF like behavior of the relaxation time, stretched exponential decay of the correlation function). These effects can be partially described in terms of an extended mode coupling theory[9, 10] introducing additional hopping processes.

There exists also various alternative descriptions[3, 11] which explain the cooperative motion of the particles inside a supercooled liquid below T_c. One of these possibilities is the spin facilitated Ising model,[11–14] originally introduced by Fredrickson and Andersen. The basic idea of all these models consists in a coarse graining of space and time scales and simultaneously a reduction of the degrees of freedom. In detail that means:

1. *Coarse graining of spatial scales.* The supercooled liquid is separated into cells in such a way that each cell contains a sufficiently large number of particles which realize a representative number of molecular motions. Thus the many body system consists of a virtual lattice with the unit size l. This lattice has no influence on the underlying dynamics of the supercooled liquid.

2. *Reduction of the degrees of freedom.* Each cell will be characterized by only one trivial degree of freedom, i.e., the cell structure enables us to attach to each cell an observable σ_j (usually denoted as spin) which

characterizes the actual dynamic state of particles inside the cell j. The usual realization is given by the local density ρ_j (particles per cell) with $\sigma_j = 0$ if $\rho_j > \bar{\rho}$ and $\sigma_j = 1$ if $\rho_j < \bar{\rho}$ where $\bar{\rho}$ is the averaged density of the system. This mapping implies consequently different mobilities of the particles inside such a cell, i.e., $\sigma_j = 0$ corresponds to the immobile solid like state and $\sigma_j = 1$ to the mobile state of cell j. The set of all spin observables $\sigma = \{\sigma_j\}$ forms a configuration. The evolution of the statistical probability distribution function $P(\sigma, t)$ can be described by a Nakajima–Zwanzig equation (or generalized master equation) by using a projection of the real dynamics to the dynamics of σ.

3. *Coarse graining of the time scale.* This step bases on the assumption that the memory term of the Nakajima–Zwanzig equation is determined by the fast molecular processes while the slow dynamics is mainly included within the local time contributions. Of course, the validity of this assumption depends strongly on the choice of the remaining degrees of freedom, and in many cases it is very hard (or impossible from the actual point of view) to give a satisfactory explantation of this assumption. However, if this separation of the dynamics is justified one can introduce an elementary time scale larger than the time scale of the fast molecular processes. Therefore, the memory term will be reduced to simple local time terms. Finally, one obtains an evolution equation which is equivalent to the mathematical representation of a usual master equation.

$$\frac{\partial P(\sigma, t)}{\partial t} = \sum_{\sigma'} L(\sigma, \sigma')\, P(\sigma, t) \tag{1}$$

The dynamical matrix $L(\sigma, \sigma')$ is determined by the above discussed formal procedure. Unfortunately, the direct calculation is mostly very complicated, so that one should use reasonable assumptions about the mathematical structure of L.

To make the time evolution of the glass configurations more transparent we use the argumentation following the idea of Fredrickson and Andersen,[11–14] i.e., we suppose that the basic dynamics is a simple process $\sigma_j = +1 \leftrightarrow \sigma_j = 0$ controlled by the thermodynamical Gibb's measure and by self induced topological restrictions. In particular, an elementary flip at a given cell is allowed only if the number of the nearest neighbored mobile cells ($\sigma_j = +1$) is equal or larger than a restriction number n with $0 < n < z$ (z: coordination number). So, elementary flip processes and geometrical restrictions lead to the cooperative rearrangement of the underlying system and therefore to a mesoscopical modelling describing a supercooled liquid below T_c. Such models[11–14] are denoted as n-spin facilitated Ising model

on a d-dimensional lattice SFM$[n, d]$. The SFM$[n, d]$ can be classified as an Ising-like model the kinetics of which is confined by restrictions of the ordering of nearest neighbors to a given lattice cell. This self-adapting environments influence in particular the long-time behavior of the spin–spin and therefore of the corresponding density–density correlation functions. These models were studied numerically[15–18] (SFM$[2, 2]$) and recently also analytically[19] (SFM$[1, 1]$).

The SFM$[1, 1]$ is the simplest model which reflects the cooperative dynamics of the spin facilitated kinetic Ising models. It is an important fact that the direct neighbors of every cell with the state $\sigma_j = +1$ can change their state. This behavior is completely independent from the state of these neighbors. In models of higher dimension, e.g., SFM$[2, 2]$, exist a finite fraction of cell with $\sigma_j = +1$ which nearest environment is blocked by the next neighbors.[18] Therefore, the SFM$[1, 1]$ is a model describing a relatively weak cooperativity. Nevertheless, this model shows a characteristic slowing down of the kinetic. On the other hand the SFM$[1, 1]$ allows various possibilities for a mathematical description discussed in the present paper. From that point of view the SFM$[1, 1]$ is a suitable model for a study of cooperative processes.

II. APPROACHES TO THE SFM[1, 1]

In this section the basis ideas are presented which will be used in the subsequent chapters for an analysis of the SFM$[1, 1]$.

A. Fock-Space Approach

Following Doi,[20] compare also ref. 21, the probability distribution $P(\sigma, t)$ can be related to a state vector $|F(t)\rangle$ in a Fock-space according to $P(\sigma, t) = \langle \sigma \mid F(t)\rangle$ and $|F(t)\rangle = \sum_\sigma P(\sigma, t)\,|\sigma\rangle$, respectively, with the basisvectors $|\sigma\rangle$. Using this representation the Master equation (1) can be transformed to an equivalent equation in a Fock-space

$$\partial_t\,|F(t)\rangle = \hat{L}\,|F(t)\rangle \tag{2}$$

The dynamical matrix $L(\sigma, \sigma')$ of (1) is mapped onto the operator $\hat{L}$ given in a second quantized form with d and $d^\dagger$ being the annihilation and creation operators, respectively, for flips processes. Usually $\hat{L}$ is expressed in terms of creation and annihilation operators which satisfy Bose commutation rules.[20, 22, 23] The SFM$[n, d]$ can be interpreted as a lattice gas ($\sigma_i = 0$: empty cell, $\sigma_i = 1$: occupied cell) with special kinetic restrictions, i.e., changes of the configuration σ are possible only under the presence of

the exclusion principle. To preserve the restriction of the occupation number in the underlying dynamical equations too, the commutation rules of the operators $\hat{d}$ and $\hat{d}^\dagger$ are those of Pauli-operators:[25, 21, 22, 26]

$$[\hat{d}_i, \hat{d}_j^\dagger] = \delta_{i,j}(1 - 2\hat{d}_i^\dagger \hat{d}_i) \qquad [\hat{d}_i, \hat{d}_j] = [\hat{d}_i^\dagger, \hat{d}_i^\dagger] = 0 \qquad \hat{d}_i^2 = (\hat{d}_i^\dagger)^2 = 0 \tag{3}$$

It should be remarked that the method can be extended to the case of higher restricted occupation numbers.[27] As it was shown by Doi[20] the average of a physical quantity $B(\sigma)$ is given by the average of the corresponding operator $\hat{B}(t) = \sum_\sigma |\sigma\rangle\, B(\sigma)\, \langle\sigma|$ via

$$\langle \hat{B}(t) \rangle = \sum_\sigma P(\sigma, t)\, B(\sigma) = \langle s|\, \hat{B}\, |F(t)\rangle \tag{4}$$

with the notation $\langle s| = \sum_\sigma \langle\sigma|$. Remark that the normalization condition is manifested in the relation $\langle s \mid F(t)\rangle = 1$. The evolution equation for an operator $\hat{B}$ can be written as

$$\partial_t \langle \hat{B}\rangle = \langle s|\, [\hat{B}, \hat{L}]\, |F(t)\rangle \tag{5}$$

Here we have used the necessary relation $\langle s|\, \hat{L} = 0$, which is an immediately consequence of the normalization condition.

The evolution operator for the one-dimensional SFM[1, 1] can be written as

$$\hat{L} = \sum_i (\hat{D}_{i+1} + \hat{D}_{i-1})[\lambda(\hat{d}_i - \hat{D}_i) + \beta(\hat{d}_i^\dagger - (1 - \hat{D}_i))] \tag{6}$$

with the particle number operator $\hat{D}_i = \hat{d}_i^\dagger \hat{d}_i$ and temperature dependent jumping rates λ and β. Applying a simple activation dynamics it results

$$\lambda = \nu^{-1} \exp(\varepsilon/T) \qquad \text{and} \qquad \beta = \nu^{-1} \exp(-\varepsilon/T)$$

where ν^{-1} is an elementary time scale (ε is the energy difference between the solid and liquid like state). The knowledge of $\hat{L}$ and the corresponding evolution equation (2) allows a reasonable analysis of the SFM[1, 1]. The method is applied further in Section III to calculate the autocorrelation function.

B. Kinetic Approach

The equilibrium state of the SFM[1, 1] at very low temperatures is characterized by a small concentration of single mobile cells, and only the two cells neighbored to such a mobile cell are able to change their orientation.

Blocks of mobile cells with a length $\ell \geqslant 2$ are extremely rare and can be neglected for the following investigations. Such blocks have only a short life time and they can be interpreted as "unstable" states. A single mobile cell, neighbored by blocks of immobile cells, can not be annihilated by a simple step because of the above mentioned restrictions. However, one can now distinguish between three types of quasi elementary local processes:

1. Diffusion. A diffusion of a single cell is possible by the following steps. An immobile cell neighbored to the mobile cell changes the state with the probability $\alpha \simeq \exp(-\varepsilon/T)$ and becomes mobile. Then, the original mobile cell changes their state to an immobile one. It results an effective diffusion of a single mobile cell, see also Fig. 1a. Thus the probability for a diffusion step is of an order of magnitude of α.

2. Creation of mobile single cell. A new single cell can be created by the following procedure. One of the two immobile cells neighbored to the single mobile cell changes their state and becomes mobile (probability α). Then, one of the two immobile cells neighbored to the mobile block of length 2 changes their state and becomes also mobile (probability α). At least, the central cell of this block becomes immobile (probability ≈ 1). One obtains two single mobile cells, separated by one immobile cell, see also Fig. 1b. The probability for the creation of a new single mobile cell in the nearest environment of another single mobile cell is of order α^2.

3. Annihilation of a single mobile cell. A single mobile cell can be neighbored by another single mobile cell, separated only by one immobile cell (probability $\rho \simeq$ density of mobile states). The immobile cell between both mobile cell changes their state (probability α). Now one obtains a mobile block of length 3. Finally, the length is reduced to 2 and then to 1 (probability 1). Thus, the probability for the annihilation of new single mobile cell in the nearest environment of another single mobile is approximately $\alpha\rho$.

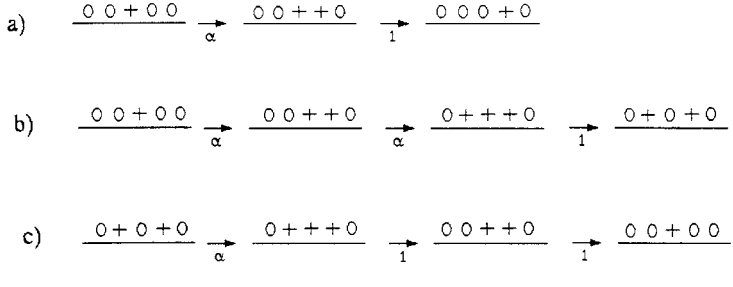

Fig. 1. Diffusion (a), creation (b), and annihilation (c) of $\sigma = 1$ states composed by elementary flip processes.

These three quasi elementary processes contribute to a conventional master equation. To find out that one, let us separate the 1-dimensional space in sufficiently large supercells containing N cells. The number of mobile spins in such a supercell i, $n_i \ll N$, can be changed by a creation of new mobile units, the annihilation of mobile units or the diffusion into a neighbored supercell. The configuration of the whole system can be described by the configuration vector $\mathbf{n} = \{n_i\}$, the probability that such a configuration is realized at the time t is denoted as $P(\mathbf{n}, t)$. The time evolution of these probabilities is given by the following master equation:

$$\begin{aligned}\frac{\partial P(\mathbf{n}, t)}{\partial t} = &\sum_i \alpha^2 [(n_i - 1)\, P(\mathbf{n} - \mathbf{r}_i, t) - n_i P(\mathbf{n}, t)] \\ &+ \sum_i \frac{\alpha}{N} [n_i(n_i + 1)\, P(\mathbf{n} + \mathbf{r}_i, t) - n_i(n_i - 1)\, P(\mathbf{n}, t)] \\ &+ \frac{1}{2} \sum_{i,j} \alpha \Theta_{ij} [(n_j + 1)\, P(\mathbf{n} + \mathbf{r}_j - \mathbf{r}_i, t) - n_j P(\mathbf{n}, t)] \end{aligned} \tag{7}$$

where the above discussed transition rates for diffusion, annihilation and creation are taken into account. The reaction vector $\mathbf{r}_i$ is defined by $r_i^\alpha = \delta_i^\alpha$. The solution of this equation (see Section IV) gives a reasonable description of the low temperature behavior of the SFM[1, 1].

C. Numerical Approach

The numerical simulation bases on the following steps. Starting from a regular (square) lattice introduced before we introduce at each lattice point a value σ_i with the two possible states $\sigma_i = 0, 1$ and the initial configuration $\sigma = \{\sigma_i = 1 \text{ for all } i\}$. We allow the elementary steps: $\sigma_i = 0 \rightleftharpoons \sigma_i = +1$. Such flips are realized with a transition probability 1 for $1 \to 0$ and $\exp\{-\varepsilon/T\}$ for $0 \to 1$ (Metropolis algorithm). In addition to this thermodynamic flip rate we have the topological restriction that a flip of cell i is only possible, if the following condition is satisfied $\sigma_{i-1} + \sigma_{i+1} > 0$. This restriction leads to the characteristic hindrance effects of the SFM[1, 1]. Using these elementary steps it is easy to create an equilibrium configuration. The equilibrium is reached if the averaged state $\bar{\sigma} = \langle \sigma_i \rangle = N_+/(N_0 + N_+)$ ($N_{+,0}$ are the numbers of cell with the state $\sigma = 1$ and $\sigma = 0$, respectively) becomes

$$\bar{\sigma} = \frac{N_+}{N_0 + N_+} \longrightarrow \bar{\sigma}_{\text{eq}} = \frac{1}{1 + \exp(\varepsilon/T)} = \frac{\beta}{\lambda + \beta} \tag{8}$$

The algorithm leads to a decay of the average $\bar{\sigma} = \langle \sigma_i \rangle$ from the initial value $\bar{\sigma}(0) = 1$ to the thermodynamical equilibrium $\bar{\sigma}(\infty) = \bar{\sigma}_{\text{eq}}$. It should be denoted that the principle of detailed balance is always fulfilled, i.e., the equilibrium state is realized for each cell and each elementary process. $\bar{\sigma}(t)$ is one of the numerical standard quantities determined here. Another quantities are related to the thermodynamical equilibrium. Because of the fact that the Hamiltonian H of the SFM[1, 1] is equivalent to a simple paramagnetic gas, i.e., $H = -\varepsilon \sum_i \sigma_i$, the equilibrium states are simple random chains with a probability $p = \bar{\sigma}_{\text{eq}}$ for to get the state $\sigma = 1$ and $q = 1 - \bar{\sigma}_{\text{eq}}$ to obtain the state $\sigma = 0$. The decay of a given equilibrium state is characterized by the relaxation time. This relaxation time can be obtained from an analysis of the time dependent normalized autocorrelation function

$$C(t) = \frac{\langle \sigma_i(t)\, \sigma_i(0) \rangle - \bar{\sigma}_{\text{eq}}^2}{\bar{\sigma}_{\text{eq}}(1 - \bar{\sigma}_{\text{eq}})} \tag{9}$$

or from the decay of the global mobility function. This is the fraction of cells $F(t)$, which remain unflipped after a time interval t from an arbitrary initial time has elapsed.[18] The numerical simulations will be used to a verification of the results obtained from the above mentioned analytical techniques.

III. SHORT-TIME BEHAVIOR

A. Relaxation into the Thermodynamical Equilibrium

The short time behavior of these relaxation is far from the equilibrium, and it can not be expected that there is a linear relation to the properties of the equilibrium via the fluctuation dissipation theorem.

1. Hierarchical Equations. The time evolution of the averaged spin state $\bar{\sigma}(t)$ can be obtained from (5) by using the identity $\bar{\sigma}(t) = \langle \hat{D}_i \rangle$ and (6). Hence

$$\partial_t \bar{\sigma} = \beta(\langle \hat{D}_{i-1} \rangle + \langle \hat{D}_{i+1} \rangle) - (\lambda + \beta)[\langle \hat{D}_{i-1} \hat{D}_i \rangle + \langle \hat{D}_{i+1} \hat{D}_i \rangle]$$

This equation includes higher moments of neighbored cells. The evolution equation of these moments contains the next higher correlations, i.e., one obtains a infinite large hierarchical system of evolution equations. The

simplest way for a breaking off of this hierarchy is the decoupling ansatz $\langle \hat{D}_{i-1}\hat{D}_i \rangle \approx \langle \hat{D}_{i-1} \rangle \langle \hat{D}_i \rangle = \bar{\sigma}^2$ which leads to the mean field solution

$$\bar{\sigma}(t) = \frac{\bar{\sigma}_{\text{eq}}}{1-(1-\bar{\sigma}_{\text{eq}})\exp(-t/\tau_0)} \tag{10}$$

with the relaxation time $\tau_0 = (\lambda+\beta)^{-1}/2$.

Another possibility bases on a more accurate decoupling[19] considering any possible block of spin down states. On the other hand, blocks containing down and up states are decoupled into products of spin averages and smaller blocks of pure down states. As a result of this procedure one obtains a infinite large system of nonlinear evolution equations which can be solved exactly. Using

$$\phi(y) = (1-\bar{\sigma}_{\text{eq}}) \int_0^y \bar{\sigma}(t)$$

one obtains nonlinear integral equation[19]

$$\int_0^\infty dy \exp\left\{ -py - \frac{\phi(y)}{p+1} \right\} = \frac{2+p-\bar{\sigma}_{\text{eq}}}{(p+1)(1+p-\bar{\sigma}_{\text{eq}})} \tag{11}$$

for the quantity ϕ. Note that p is a free parameter, i.e., (11) must be fulfilled for all $p>0$. The knowledge of ϕ allows the determination of $\bar{\sigma}(t)$ due to the relation $\sigma(t)(1-\bar{\sigma}_{\text{eq}})^{-1}\dot{\phi}(t)$.

For the short time regime one gets:[19]

$$\bar{\sigma}(t) = \bar{\sigma}_{\text{eq}} + 2(1-\bar{\sigma}_{\text{eq}})\exp\{-t/\tau_0\}\frac{\mathrm{I}_1(t/t_0)}{t/t_0} \tag{12}$$

Here $\mathrm{I}_1(x)$ is the first order modified Bessel function and t_0 is a second relaxation constant defined by $t_0^{-1} = 4\sqrt{\lambda\beta}$. Figure 2 shows the numerical decay of $\bar{\sigma}(t)$ obtained from the above mentioned numerical simulations in comparison with (10) and (12), respectively. It can be seen, that both formulas approach only the short time regime very well. The actual differences between numerical simulations and (10) and (12), respectively, show (see Fig. 3) that a fit based on (10) gives rise to a slightly larger error that the fit with (12). Thus, we conclude that the result (12) is more appropriate for the short time regime than (10). Note that this statement is valid for each temperature $T>0$.

The difference between both results consists in the fact that the mean field approximation (10) suppresses the fluctuations of neighbored spins

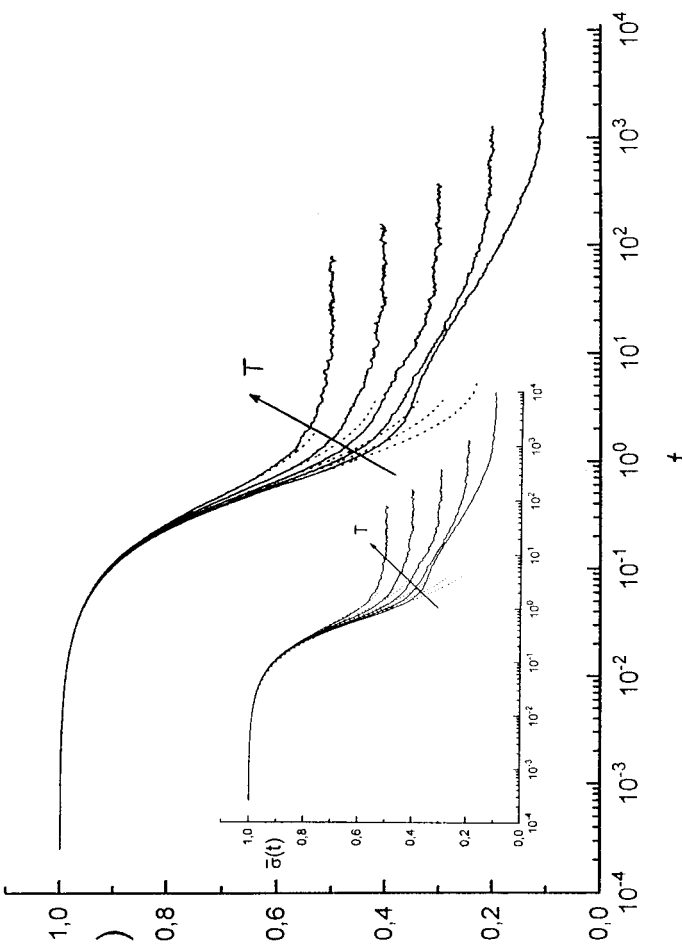

Fig. 2. Short time behavior of $\bar{\sigma}(t)$: Numerical simulations in comparison with the predictions of Eq. (12) for various temperatures corresponding to $\bar{\sigma}_{eq} = 0.1$, 0.2, 0.3, 0.4, and 0.5 with $\varepsilon/T = \ln(\bar{\sigma}_{eq}^{-1} - 1)$. The temperature increases in the direction of the arrow. The dotted lines corresponds to the theoretical predictions. The insert shows the same data fitted by the mean field predictions of Eq. (10).

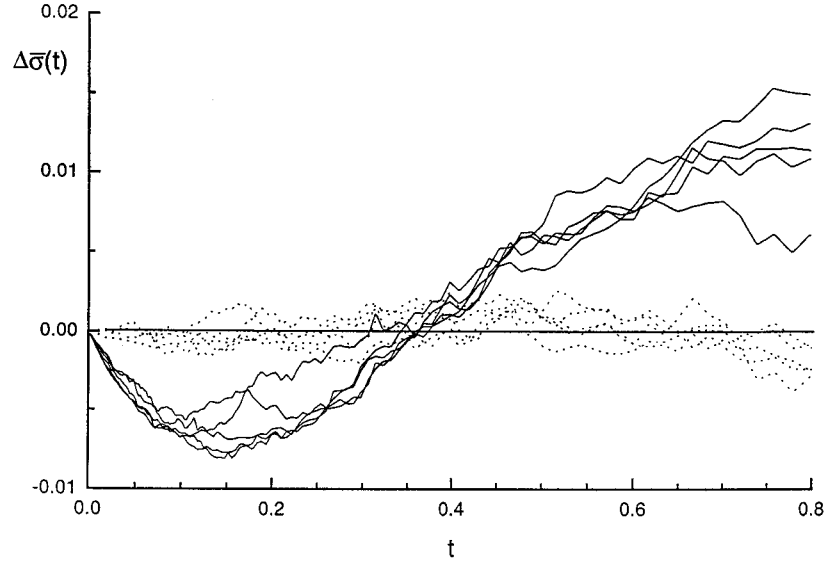

Fig. 3. Difference (short time regime) $\Delta\bar{\sigma}(t)=\bar{\sigma}(t)-\bar{\sigma}_{\text{num}}(t)$ between the predictions of Eq. (10) and numerical data (full lines) and between the predictions of Eq. (12) and numerical data (dotted lines), respectively, for $\bar{\sigma}_{\text{eq}}=0.1,...,0.5$. There is no significant dependence on $\bar{\sigma}_{\text{eq}}$. But it can be observed that the mean field approximation Eq. (10) shows a systematic deviation from the numerical data, whereas the differences of the second approach Eq. (12) are mainly fluctuations caused by the numerical simulation. Obviously, the accuracy of the simple mean field theory is smaller.

completely whereas the solution (12) takes these fluctuations into account at least partially.

2. Exact Solution for $T=0$. The zero temperature case can be solved exactly. To this aim we define the cluster function

$$\hat{\Psi}_i^m=\prod_{j=0}^{m}\hat{D}_{i+j}\equiv\hat{D}_i\hat{D}_{i+1}\cdots\hat{D}_{i+m}$$

Such a function gives only a nonzero contribution when all the $m+1$ cells of the cluster are in the state $\sigma=1$. Using the algebraic properties of the Pauli-operators we are able to derived an exact evolution equation[19] for the average of the cluster function $\langle\hat{\Psi}_i^m\rangle$. Obviously there occurs a hierarchy of equation where $\hat{\Psi}_i^m$ is related to higher order cluster functions. However for the zero temperature limit where the stationary value $\bar{\sigma}=\beta/(\lambda+\beta)$, see (8) tends to zero the set of equations reads

$$\partial_t\langle\Psi^m\rangle=-m\langle\Psi^m\rangle-\langle\Psi^{m+1}\rangle$$

where we have dropped the cell number due to translational invariance. Furthermore the time variable is rescaled by $t \to t/\tau_0$. As the initial condition we choose again a parallel alignment $\langle \Psi^m \rangle (t=0) = 1$ corresponding to complete liquid-like state. The last equation can be solved by the ansatz $\langle \Psi^m \rangle = \varphi^m(t) \exp(-mt)$ leading to

$$\partial_t \varphi^m = \varphi^{m+1} \exp(-t)$$

The solution of the last equation can be easily calculated under the initial condition. As result we get the final relation

$$\langle \Psi^m \rangle (t) = \exp\left\{-m \frac{t}{\tau_0}\right\} \exp\left\{\exp\left(-\frac{t}{\tau_0}\right) - 1\right\} \tag{13}$$

The cluster function reveals a double exponential decay. In the initial time scale the conventional exponential decay dominates. However in the long time limit it results a pronounced slowing down leading to a nonergodic behavior which is manifested in finite value for $\bar{\sigma}(t) = \langle \Psi^0(t) \rangle$ in the limit $t \to \infty$. We find $\bar{\sigma}(\infty) = e^{-1}$. The exact result is depicted in Fig. 4. The comparison with simulations reveal that the numerically determined decay of $\bar{\sigma}(t)$ coincides with Eq. (13) ($m=0$) only for an intermediated time scale for low temperatures.

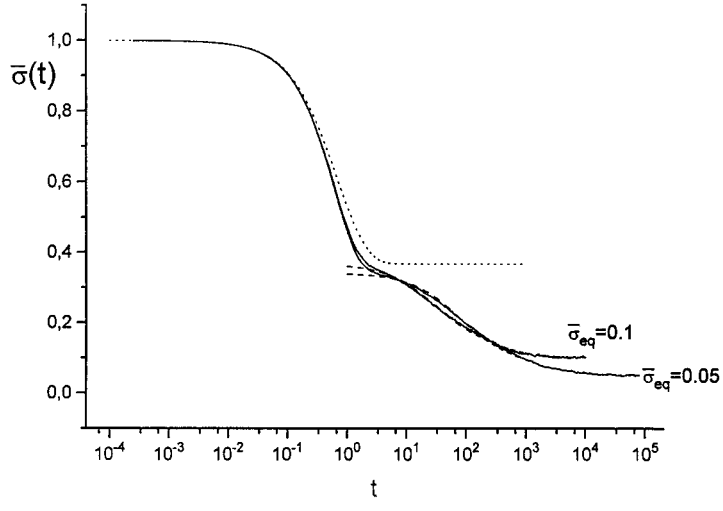

Fig. 4. Decay of $\bar{\sigma}(t)$ for very low temperatures (corresponding to $\bar{\sigma}_{eq} = 0.05$ and 0.1). The dotted line is the to rigorous solution for $T=0$ Eq. (13). The dashed lines are the theoretical predictions obtained from Eq. (25) and the application of the fluctuation dissipation theorem.

B. Equilibrium Relaxation Behavior

An analytical determination of the density autocorrelation function (9) can be realized by using the relation

$$C(t) = \langle \hat{\eta}_i(t)\, \hat{\eta}_i(0) \rangle = \langle \hat{\eta}_i e^{\hat{L}t} \hat{\eta}_i \rangle \tag{14}$$

which follows immediately from the above discussed Fock space representation, compare Eq. (2). Here we have introduced for convenience the operator

$$\hat{\eta}_i = \frac{\hat{D}_i - \bar{\sigma}_{\text{eq}}}{\sqrt{\bar{\sigma}_{\text{eq}}(1-\bar{\sigma}_{\text{eq}})}}$$

To calculate the correlation function Eq. (14) we use an expansion in powers of the time

$$C(t) = \sum_k \frac{(-t/2\tau_0)^k}{k!} \Gamma_k \qquad \text{with} \quad \Gamma_k = (-2\tau_0)^k \langle \hat{\eta}_i \hat{L}^k \hat{\eta}_i \rangle \tag{15}$$

(the time scale τ_0 is defined again by $\tau_0 = (\lambda+\beta)^{-1}/2$). Using the algebraic properties of the Pauli-operators and the abbreviation $\hat{l}_i = \lambda(\hat{d}_i - \hat{D}_i) + \beta(\hat{d}_i^{\dagger} - (1-\hat{D}_i))$ we get some helpful auxiliary relations

$$\langle s|\, \hat{l}_i = 0, \quad \langle s|\, \hat{\eta}_i \hat{l}_i = -\frac{1}{2\tau_0} \langle s|\, \hat{\eta}_i \quad \text{and} \quad \langle s|\, \hat{D}_i \hat{l}_i = -\frac{\sqrt{\bar{\sigma}_{\text{eq}}(1-\bar{\sigma}_{\text{eq}})}}{2\tau_0} \langle s|\, \hat{\eta}_i \tag{16}$$

Applying these relations and

$$\langle s|\, \hat{\eta}_i \hat{D}_i = \sqrt{\frac{1-\bar{\sigma}_{\text{eq}}}{\bar{\sigma}_{\text{eq}}}} \langle s|\, \hat{D}_i \qquad \text{and} \qquad \langle s|\, \hat{D}_i^2 = \langle s|\, \hat{D}_i$$

the correlation function $C(t)$ can be represented by diagrams. Denoting the operator $\hat{\eta}_i$ by an open circle $\circ$ and the operator $\hat{D}_i$ by a bullet $\bullet$ the terms $\langle s|\, \hat{\eta}_i \hat{L}^k$ can be simply figured by chains of circles and bullets. The zero order ($k=0$) corresponds to one open circle representing $\hat{\eta}_i$. The first order diagrams are created from an application of $\hat{L} = \sum_m (\hat{D}_{m-1} + \hat{D}_{m+1})\, \hat{l}_m$ applied on the state $\langle s|$ (into the left direction). Nonvanishing contributions result only for $m=i$. It remains $\langle s|\, \hat{\eta}_i \hat{L} = -(\langle s|\, \hat{\eta}_i \hat{D}_{i-1} + \langle s|\, \hat{\eta}_i \hat{D}_{i+1})/(2\tau_0)$ corresponding to two diagrams (see Fig. 5). The bullet stands the operator $\hat{D}_{i\pm1}$ neighbored to the operator $\hat{\eta}_i$ (open circle). The next application of $\hat{L}$ on $\langle s|\, \hat{\eta}_i \hat{D}_{i-1}$ and $\langle s|\, \hat{\eta}_i \hat{D}_{i+1}$, respectively, leads to 2×4 new diagrams,

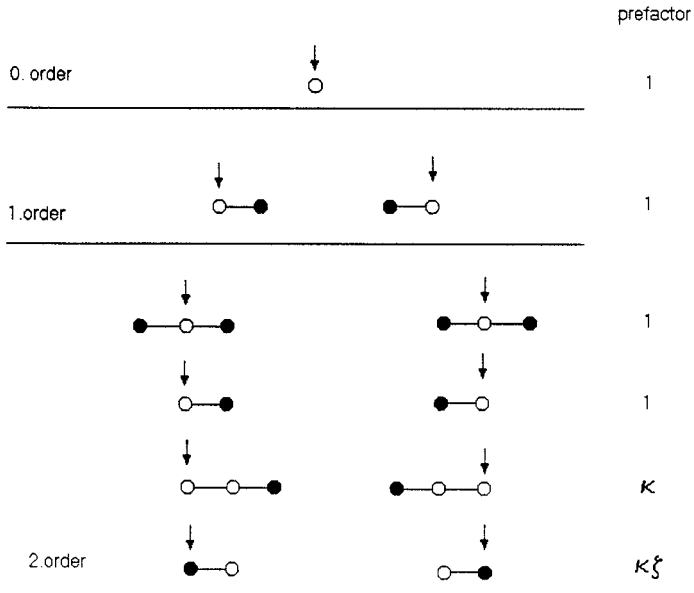

Fig. 5. Diagram expansion of $\langle s|\,\hat{\eta}_i\hat{L}^k$ for $k=0\cdots 2$. The arrow indicates the initial point. The prefactors are products of 1, $\kappa=(\bar{\sigma}_{\rm eq}(1-\bar{\sigma}_{\rm eq}))^{1/2}$ and $\zeta=((1-\bar{\sigma}_{\rm eq})/\bar{\sigma}_{\rm eq})^{1/2}$.

because both cases $m=i$ and $m=i\pm 1$ leads to nonvanishing contributions. The structure of all these diagrams are drawn in Fig. 5. The generalization of this first steps lead to the following rules:

1. For a given diagram in any order, the next higher order can be constructed by picking out a point ($\circ$,$\bullet$) and the subsequent transformation of this point into $\circ$. The diagram should be multiplied by a prefactor 1 for the transformation $\circ\to\circ$ and by a prefactor $\sqrt{\bar{\sigma}_{\rm eq}(1-\bar{\sigma}_{\rm eq})}$ in case of the transformation $\circ\to\bullet$. Denoted that all changes of signs and all powers of $(1/2\tau_0)$ are taken into account, see the representation (15).

2. Simultaneously, a neighbored point is picked out and transformed into $\bullet$. The diagram is multiplied by the factor

- $\sqrt{(1-\bar{\sigma}_{\rm eq})/\bar{\sigma}_{\rm eq}}$ if the original point was $\circ$.
- 1 if the original point was $\bullet$.
- 1 if the original point was an empty point (at the end of the chains).

Following (15) all diagrammatic contributions are multiplied by $\hat{\eta}_i$ and the average procedure over all points should be performed. Because of the paramagnetic Hamiltonian (see above) the average over an arbitrary chain, e.g., $\langle\ldots\hat{\eta}_{i-2}\hat{D}_{i-1}\hat{\eta}_i\hat{D}_{i+1}\ldots\rangle$ decays in a chain of single averages,

e.g., $\ldots\langle\hat{\eta}_{i-2}\rangle\langle\hat{D}_{i-1}\rangle\langle\hat{\eta}_i\rangle\langle\hat{D}_{i+1}\rangle\ldots$. Because of $\langle\hat{\eta}_m\rangle = 0$ only diagrams with a single circle becomes a nonzero value (Note that $\langle\hat{\eta}_i^2\rangle = 1$ and $\langle\hat{D}_i\rangle = \bar{\sigma}_{\text{eq}}$) if this circle is localized at the original position i.

The application of the diagram rules allows a successive determination of the coefficients Γ_k in (15). Unfortunately, the number of diagrams increases rapidly and a systematical evaluation becomes impossible. Therefore, it will be helpful to find a reasonable approximation of the autocorrelation function $C(t)$. Here we present some few possible standard methods, which allow a determination of $C(t)$ at least for short times.

- Taylor Expansion:

The simplest approach consists of a breakdown of the series at a given order, i.e. one obtains the finite Taylor expansion

$$C(t) \approx \sum_{k=0}^{S} \frac{(-t/2\tau_0)^k}{k!}\,\Gamma_k \tag{17}$$

The coefficients Γ_k can be determined by the above discussed procedure. For the lowest order follows

$$\Gamma_0 = 1 \qquad \Gamma_1 = 2\bar{\sigma}_{\text{eq}} \qquad \Gamma_2 = 2\bar{\sigma}_{\text{eq}}(1+\bar{\sigma}_{\text{eq}}) \qquad \Gamma_3 = 4\bar{\sigma}_{\text{eq}}(1+\bar{\sigma}_{\text{eq}})$$

and

$$\Gamma_4 = 10\bar{\sigma}_{\text{eq}} + 18\bar{\sigma}_{\text{eq}}^2 - 16\bar{\sigma}_{\text{eq}}^3 + 4\bar{\sigma}_{\text{eq}}^4$$

The insert of Fig. 6 shows the behavior of the autocorrelation function $C(t)$ for $S = 1\cdots 4$. The series reflects very well the short time behavior with increasing S. However, the convergence of these series at moderate and large time scales is weak.

- Cumulant Expansion:

This expansion has the representation:

$$C(t) = \exp\left\{\sum_{k=1}^{S} \frac{(-t/2\tau_0)^k}{k!}\,\gamma_k\right\} \tag{18}$$

The first cumulants γ_k can be obtained from the by a simple calculation from the coefficients Γ_k:

$$\gamma_1 = 2\bar{\sigma}_{\text{eq}} \qquad \gamma_2 = 2\bar{\sigma}_{\text{eq}}(1-\bar{\sigma}_{\text{eq}}) \qquad \gamma_3 = 4\bar{\sigma}_{\text{eq}}(1-\bar{\sigma}_{\text{eq}})^2$$

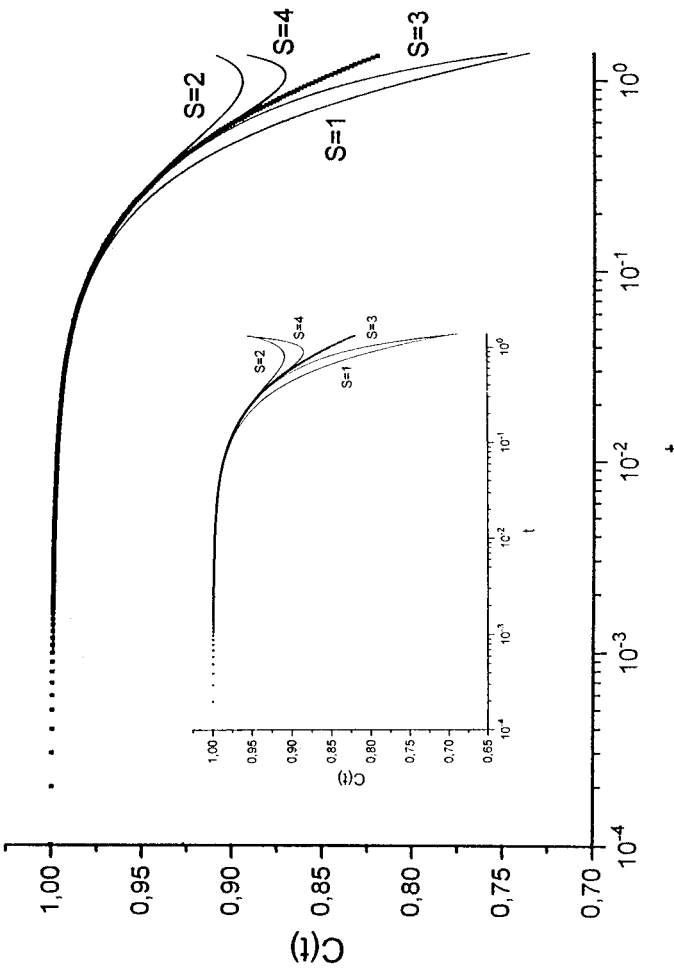

Fig. 6. Short time behavior of the first finite cumulant series ($S = 1 \ldots 4$) of the SFM[1, 1] for $\bar{\sigma}_{eq} = 0.1$ in comparison with the corresponding numerical simulation. The insert presents the first finite Taylor series. The accuracy shows for both cases only a slight increase with increasing S.

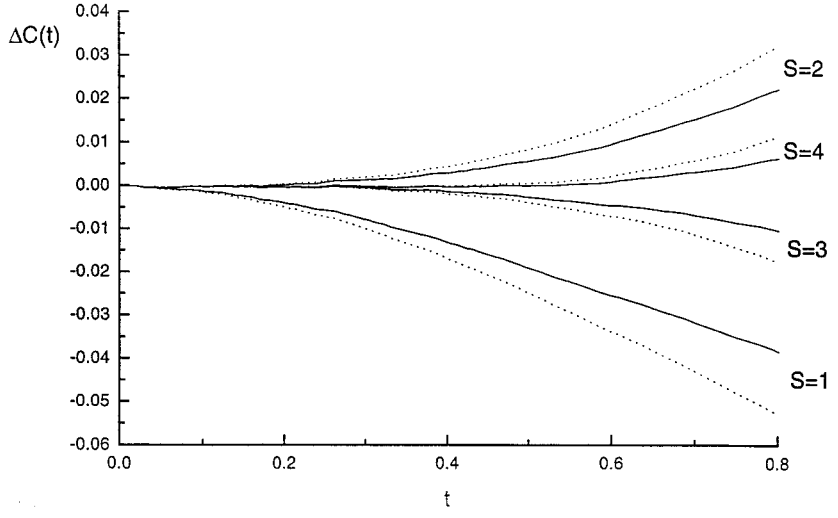

Fig. 7. Deviations of the first finite Taylor series (dotted lines) and the first finite cumulant series (full lines), respectively, from the numerical data for $\bar{\sigma}_{eq} = 0.1$. The accuracy of the cumulant series is slightly better than the Taylor expansion of the same order.

and

$$\gamma_4 = 2\bar{\sigma}_{eq}(1-\bar{\sigma}_{eq})(5-8\bar{\sigma}_{eq}+4\bar{\sigma}_{eq})$$

Figure 6 shows the approximation for $C(t)$ on the short time scale using (18). From this point of view, both, Taylor expansion and Cumulant expansion, seem to be very similar. But it can be checked from the difference between the numerical simulation and (17) and (18), respectively (see Fig. 7), that the approximation (18) is slightly better than that one based on (17). However, this expansion fails also at sufficiently large times because of the weak convergence for $t \to \infty$.

- Partial summation:

Another possibility is the computation of the infinite series (15) by using reasonable approximations of the Γ_k for sufficiently large k. One obtains after some calculations (see Appendix A) the final expression for the correlation function:

$$C(t) = \sum_{n=1}^{\infty} \bar{\sigma}_{eq}^{n-1} \frac{\Gamma^2(n)}{\Gamma(2n-1)} \sum_{\mu}^{n-1} \frac{(-1)^{n-1-\mu}}{(n-1-\mu)!\,(\mu)!} \sum_{k=0}^{\infty} \frac{(2\mu)^k}{k!} \left(-\frac{t}{\tau_0}\right)^k \qquad (19)$$

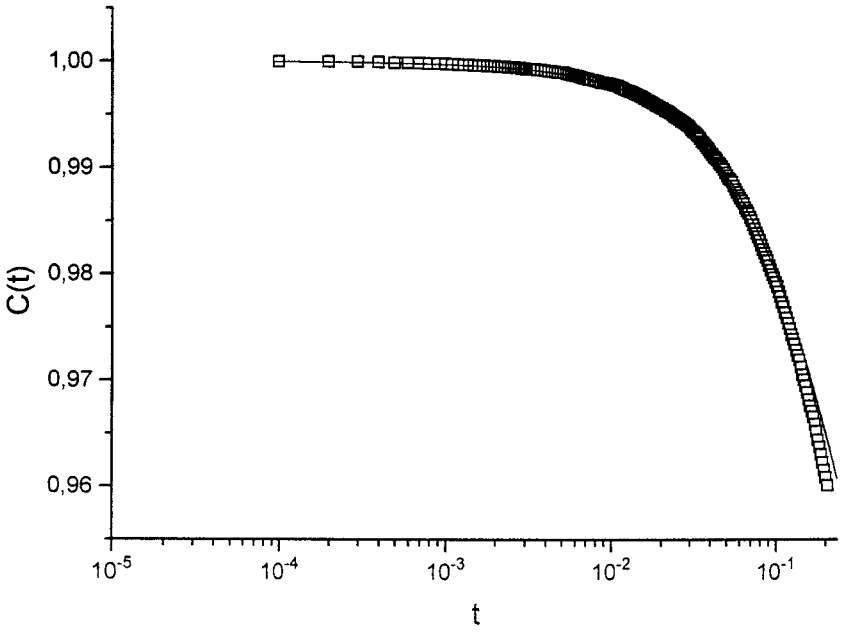

Fig. 8. Short time behavior of the partial sum of diagrams (see Eq. (22)) for the case $\bar{\sigma}_{eq} = 0.1$ in comparison with the corresponding numerical simulation. The accuracy is approximately the same as for Taylor and cumulant expansion, respectively.

Figure 8 suggests that this correlation function is also in a good agreement with the short time regime of the corresponding numerical simulations.

All presented methods show approximately the same accuracy. We obtain a sufficiently good approach to the actual numerical data for short times, but the deviation from the simulation results increases with increasing time. Obviously, the nearest environment of a given spin determines the short-time behavior of $C(t)$. This environment is reflected in the first Taylor coefficients and cumulants, respectively. On the other hand, the local environment determines the mean contributions of the expansion (19) for short times. On the other hand, the long–time behavior of the autocorrelation function $C(t)$ is significantly controlled by the spins of a large environment. Hence, finite Taylor series or cumulant expansions become invalid with increasing time. But also the some few assumptions used for the derivation of (19) are too strong for a sufficient description of the complex cooperatively rearrangement of the spins. The behavior at moderate and long times must be described by another techniques which are presented in the following section.

IV. LONG TIME BEHAVIOR

A. Equilibrium Relaxation Behavior

1. Autocorrelation Function. The long time behavior can be obtained from a solution of (7). Although this equation was originally derived for sufficiently low temperatures one finds also a good agreement between the solution of (7) and numerical simulations. But it should be remarked that this equation is a very accurate approximation for long time limit because the deviation of (7) bases mainly on the balance at large scales. After the transformation

$$n_i = N\bar{\rho} + \sqrt{N}\,\xi_i$$

and the usual van Kampen system size expansion,[28] one obtains:

$$\begin{aligned}
\frac{\partial P(\xi,t)}{\partial t} &= \sum_i \alpha^2 \sum_{m_i=1}^{\infty} \frac{(-\sqrt{N})^{-m_i}}{m_i!}\left(\frac{\partial}{\partial \xi_i}\right)^{m_i}\left[(N\bar{\rho}+\sqrt{N}\,\xi_i)\,P(\xi,t)\right] \\
&+ \sum_i \alpha \sum_{m_i=1}^{\infty} \frac{N^{-m_i/2-1}}{m_i!}\left(\frac{\partial}{\partial \xi_i}\right)^{m_i} \\
&\times \left[(N\bar{\rho}+\sqrt{N}\,\xi_i)(N\bar{\rho}+\sqrt{N}\,\xi_i-1)\,P(\xi,t)\right] \\
&+ \sum_{i,j} \alpha\Theta_{ij} \sum_{m_i,k_j=0}^{\infty\prime} \frac{(-1)^{m_i} N^{-(m_i+k_j)/2}}{m_i!\,k_j!} \\
&\times \left(\frac{\partial}{\partial \xi_i}\right)^{m_i}\left(\frac{\partial}{\partial \xi_j}\right)^{k_j}\left[(N\bar{\rho}+\sqrt{N}\,\xi_j)\,P(\xi,t)\right]
\end{aligned}$$

Note, that the sum $\sum'$ excludes the case $m_i = k_j = 0$. The expansion in terms of $1/\sqrt{N}$ leads up to the first two orders

$$\begin{aligned}
\frac{\partial P(\xi,t)}{\partial t} &= \sum_i \alpha^2 \left\{ -\sqrt{N}\,\bar{\rho}\,\frac{\partial P(\xi,t)}{\partial \xi_i} - \frac{\partial(\xi_i P(\xi,t))}{\partial \xi_i} + \frac{\bar{\rho}}{2}\frac{\partial^2 P(\xi,t)}{\partial \xi_i^2} \right\} \\
&+ \sum_i \alpha \left\{ \sqrt{N}\,\bar{\rho}^2 \frac{\partial P(\xi,t)}{\partial \xi_i} + 2\bar{\rho}\,\frac{\partial(\xi_i P(\xi,t))}{\partial \xi_i} + \frac{\bar{\rho}^2}{2}\frac{\partial^2 P(\xi,t)}{\partial \xi_i^2} \right\} \\
&+ \sum_{i,j} \alpha\Theta_{ij} \left\{ \frac{\partial((\xi_i-\xi_j)\,P(\xi,t))}{\partial \xi_i} + \frac{\bar{\rho}}{2}\left[\frac{\partial}{\partial \xi_i} - \frac{\partial}{\partial \xi_j}\right]^2 P(\xi,t) \right\}
\end{aligned}$$

The first order terms ($\sim\sqrt{N}$) are cancelled by using the condition $\bar{\rho}=\alpha$ which corresponds to the thermodynamical equilibrium $\langle n_i\rangle/N=\alpha$. Thus, it remains a Fokker–Planck equation for the fluctuations ξ:

$$\frac{\partial P(\xi,t)}{\partial t}=\sum_i\left[(2\alpha^2+\alpha^3)\frac{\partial^2 P(\xi,t)}{\partial\xi_i^2}-\alpha^2\left(\frac{\partial}{\partial\xi_{i+1}}\frac{\partial}{\partial\xi_i}+\frac{\partial}{\partial\xi_{i-1}}\frac{\partial}{\partial\xi_i}\right)\right]P(\xi,t)$$
$$+\sum_i\alpha^2\frac{\partial(\xi_i P(\xi,t))}{\partial\xi_i}+\sum_{i,j}\alpha\Theta_{ij}\frac{\partial((\xi_i-\xi_j)\,P(\xi,t))}{\partial\xi_i} \tag{20}$$

Using

$$A_i(\xi)=-\alpha^2\xi_i+\alpha(\xi_{i+1}+\xi_{i-1}-2\xi_i)$$

and

$$B_{ij}=\frac{1}{\sqrt{2}}(\alpha^{3/2}+\sqrt{\alpha^3+4\alpha^2})\,\delta_{i+1,j}-\frac{1}{\sqrt{2}}(\sqrt{\alpha^3+4\alpha^2}-\alpha^{3/2})\,\delta_{ij}$$

with

$$\tfrac{1}{2}(\mathbf{B}\mathbf{B}^T)_{ik}=\tfrac{1}{2}B_{ij}B_{kj}=[\alpha^3+2\alpha^2]\,\delta_{i,k}-\alpha^2(\delta_{i-1,k}+\delta_{i+1,k})$$

(20) can be rewritten as:

$$\frac{\partial P(\xi,t)}{\partial t}=-\sum_i\frac{\partial(A_i(\xi)\,P(\xi,t))}{\partial\xi_i}+\frac{1}{2}\sum_{i,k}\frac{\partial}{\partial\xi_i}\frac{\partial}{\partial\xi_k}[(\mathbf{B}\mathbf{B}^T)_{ik}\,P(\xi,t)]$$

i.e., one obtains the corresponding stochastic equation of motion:[29]

$$\frac{d\xi_m}{dt}=A_m(\xi)+\sum_n B_{mn}\eta_n(t)$$

The noise field $\eta_n(t)$ can be realized by a set of independent normalized Gaussian processes. A simple discrete Fourier transformation

$$\xi_m=\int_{-\pi}^{\pi}\frac{dq}{2\pi}\,\xi(q)\exp\{imq\}\Leftrightarrow\xi(q)=\sum_{m=-\infty}^{\infty}\exp\{-imq\}\;\xi_m$$

leads to

$$\frac{d\xi(q)}{dt}=-\Omega(q)\,\xi(q)+I(q,t)$$

with the frequencies

$$\Omega(q) = [\alpha^2/2 + \alpha] - 2\alpha \cos q = \alpha^2/2 + 2\alpha \sin^2(q/2)$$

and the noise term:

$$I(q, t) = \left[\frac{1}{\sqrt{2}} (\alpha^{3/2} + \sqrt{\alpha^3 + 4\alpha^2}) \exp(iq) - \frac{1}{\sqrt{2}} (\sqrt{\alpha^3 + 4\alpha^2} - \alpha^{3/2}) \right] \eta(q, t)$$

Under consideration of the normalized noise $\langle \eta(q, t')\, \eta^*(q', \tau') \rangle = 2\pi\delta(q - q')$ $\delta(t' - \tau')$ the correlations of $I(q, t)$ become simply $\langle I(q, t')\, I^*(q', \tau') \rangle = 4\pi\alpha\Omega(q)\, \delta(q - q')\, \delta(t' - \tau')$. Therefore, the correlation function of the fluctuations $\xi(q, t)$ can be written as:

$$\langle \xi(q, t)\, \xi^*(q', \tau) \rangle = 2\pi\alpha \exp(-\Omega(q)\, |t - \tau|)\, \delta(q - q')$$

Finally, the local correlation becomes

$$\begin{aligned} \langle \xi(r, t)\, \xi(r, 0) \rangle &= \left(\frac{1}{2\pi} \right)^2 \int_{-\pi}^{\pi} \int_{-\pi}^{\pi} dq\, dq'\, \langle \xi(q, t)\, \xi^*(q', 0) \rangle \\ &= \frac{\alpha}{2\pi} \int_{-\pi}^{\pi} \exp(-\Omega(q)\, |t|)\, dq \end{aligned}$$

Using $\Omega(q) \approx \alpha(\alpha + q^2)/2$, the last integral leads to a simple expression:

$$\langle \xi(r, t)\, \xi(r, 0) \rangle = C \exp\left(-\frac{\alpha^2 t}{2} \right) \frac{\Phi(\pi \sqrt{\alpha t/2})}{\sqrt{t}} \tag{21}$$

Φ is the error function. It is obviously that the fluctuations (21) behave like the autocorrelation function $C(t)$, see (9). On the other hand, the kinetic coefficients for creation, annihilation and diffusion processes are determined with respect to the order of magnitude, i.e., it is reasonable to expect a more generalized representation for the autocorrelation function:

$$C(t) = \exp\left(-\frac{\alpha_1^2 t}{2} \right) \frac{\Phi(\pi \sqrt{\alpha_2 t/2})}{\sqrt{2\pi\alpha_2 t}} \tag{22}$$

This representation takes into account that the time scale of the original equation (7) must not correspond to the actual time scale, e.g., the number of Monte-Carlo steps in the numerical simulations. The introduction of another time scale leads to the rescaling $t \to \mu t$. Thus, the prefactor μ generates the different coefficients $\alpha_1 = \alpha \sqrt{\mu}$ and $\alpha_2 = \alpha\mu$ because of the different coupling between t and α in the first and the second term of (21).

Furthermore, the introduction of different parameters α_1 and α_2 considers also the correct prefactors (of the transition rates) which are originally neglected in course of the derivation of Eq. (7). However, all scaling factors are simple constants, i.e., the ratio α_1/α_2 must be temperature-independent.

$C(t)$ is normalized to be the unit for $t=0$. Figure 9 shows the decay of the autocorrelation function $C(t)$ determined by numerical simulations and fitted by using (22). As expected, there is a sufficient agreement between the numerical data and the relation (22). It should be remarked that from the fit procedure follows that both parameters α_1 and α_2 are simply Arrhenius activated. The ratio α_1/α_2 depends not on the temperature, i.e., one obtains $\alpha_1/\alpha_2 = 87.29(1 \pm 0.057)$ for all values of $\bar{\sigma}_{eq}$.

2. Global Mobility $F(t)$. The global memory function can be obtained by a simple approximation. Each equilibrium state consist of local (cell) states which are independently from the states of the neighbored cells. Thus, the probability to find a chain of ξ neighbored cell with the state $\sigma = 0$ is an exponential distribution (note that $p(\xi) = \bar{\sigma}_{eq}(1-\bar{\sigma}_{eq})^{\xi} \sim \exp\{-\xi/\xi_0\}$

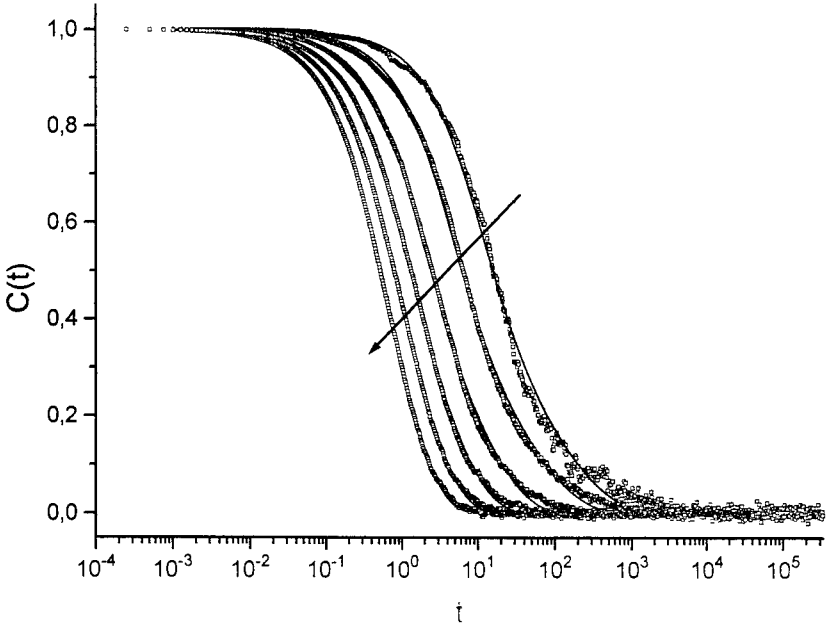

Fig. 9. Long time behavior of $C(t)$: Numerical simulations in comparison with the prediction of Eq. (25) (dotted lines, which are partially covered up by the numerical results) for various temperatures corresponding to $\bar{\sigma}_{eq} = 0.05$, 0.1, 0.2, 0.3, 0.4, and 0.5. The temperature increases in the direction of the arrow.

with $\xi_0 = -1/\ln(1-\bar{\sigma}_{eq})$). A change of the state of the chain cells is not possible by the kinetics of the cells inside the chain. Only the dynamics at the two borders leads to a decay of the self blocked chain. The motion of the two ends of the chain (characterized by the state $\sigma = 1$) can be described by the above discussed diffusive motion. The averaged penetration length at the time t of these endpoints into the original chain is given by $\xi' \simeq \sqrt{\alpha t}$. Therefore, all original chains with $\xi < \xi'$ are rebuilded whereas chains with $\xi > \xi'$ contains a remaining part of the averaged length $\Delta\xi = \xi - \xi'$ which has never changed the state of the containing cells. Therefore, the fraction of all cells which remain unflipped after the time interval t from an arbitrary initial time can be written as:

$$F(t) = \frac{\int_{\sqrt{\alpha t}}^{\infty} [\xi - \sqrt{\alpha t}] \exp\{-(\xi/\xi_0)\}\, d\xi}{\int_0^{\infty} \xi \exp\{-(\xi/\xi_0)\}\, d\xi} = \exp\left\{-\frac{\sqrt{\alpha t}}{\xi_0}\right\} \tag{23}$$

Figure 10 shows the long time behavior of $F(t)$ obtained from numerical simulations and fitted by using (23). It can be seen that the approach

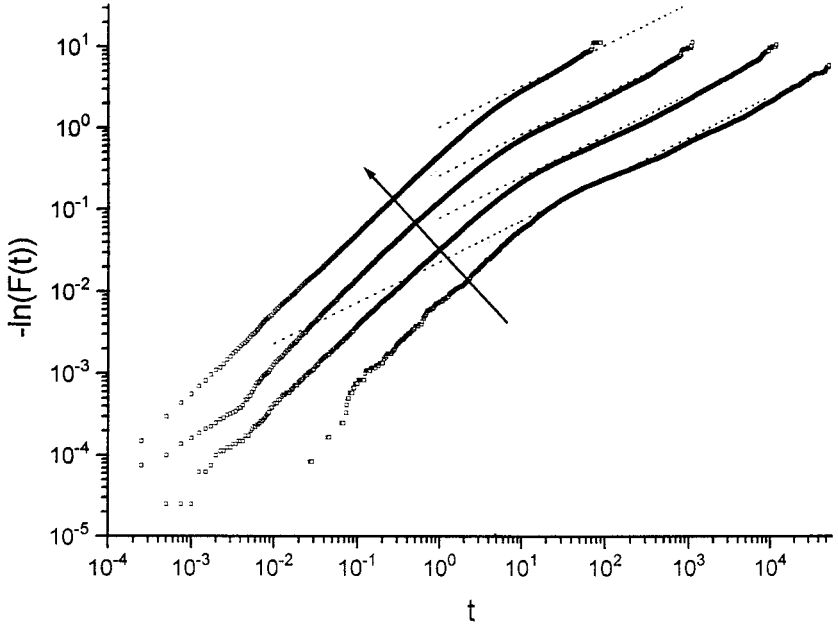

Fig. 10. Long time behavior of $F(t)$: Numerical simulations in comparison with the prediction of Eq. (26) (dotted lines) for various temperatures corresponding to $\bar{\sigma}_{eq} = 0.05$, 0.1, 0.2, and 0.4. The temperature increases in the direction of the arrow.

$\ln F(t) \sim -\sqrt{t}$ is preferred for sufficient low temperatures and at sufficient long times. Obviously, it must be considered that for short times the decay of the cells with the state $\sigma = 1$ leads to an additional contribution. Thus, the initial behavior of $\ln F(t)$ shows an approximately linear decay, i.e., $\ln F(t) \sim -t$. Furthermore, the above used assumption of a diffusion controlled decay of the chains with $\sigma = 0$ becomes relevant for sufficiently large blocks, i.e., for sufficiently low temperatures.

B. Relaxation into the Equilibrium

This behavior can be discussed briefly. Because of the fluctuation dissipation theorem there is a direct connection between the autocorrelation function $C(t)$ and the relaxation into the equilibrium. Especially the long time behavior of $\bar{\sigma}(t)$ for sufficiently long times (i.e., closed to the equilibrium state $\bar{\sigma}(t) \approx \bar{\sigma}_{\text{eq}}$) behaves like $C(t)$. It is easy to show that the behavior after reaching the quasi frozen plateau can be described also by

$$\bar{\sigma}(t) = \sigma_0 \exp\left(-\frac{\alpha_1^2 t}{2}\right) \frac{\Phi(\pi\sqrt{\alpha_2 t/2})}{\sqrt{2\pi\alpha_2 t}} \tag{24}$$

Figure 4 shows the numerically determined decay of $\bar{\sigma}(t)$ in comparison with a fit using Eq. (24). One obtains a good agreement between the predicted long time behavior ($t > 10^1$) of $\bar{\sigma}(t)$ and the numerical data.

V. CONCLUSION

As discussed above by various analytical and numerical results, the SFM[1, 1] allows both a qualitative and a quantitative study of cooperativity.[5] Therefore, the one dimensional spin facilitated kinetic Ising model is a reasonable model which offers insight into the origin of the typical slowing down in supercooled liquids by a detailed The main properties of a supercooled liquid below T_c (of MCT) can be observed very well, e.g., a stretched exponential decay of autocorrelation functions and a characteristic crossover between the low and the high temperature regime.

But it should be denoted that such a simple kinetic model like the SFM[1, 1] does not reflect all properties of the glassy dynamics, e.g., there is no fast β-process. However, the cooperative rearrangement is an intrinsic property which gives reasons for the use of the SFM[1, 1] as an model for a supercooled liquid.

An approximately exponential decay exists at sufficiently high temperatures. This can be explained by the large number of relatively local

processes. Chains of blocked states (i.e., chains of cell with the state $\sigma = 0$) are very short. Therefore, the dynamics of the SFM[1, 1] is similar to the dynamics of a paramagnetic gas. Nevertheless, the SFM[1, 1] becomes not equivalent to the paramagnetic gas because the geometrical restrictions remains effective also for $T \to \infty$, i.e., the cooperativity becomes small at high temperatures but it disappears not.

The behavior of the SFM[1, 1] for low temperatures is significant different from that of the high temperature regime. The averaged length of blocked chains increases rapidly with decreasing temperature and the diffusion controlled decay of this chains becomes relevant. The change from an approximately local dynamics to a diffusion controlled dynamics is reflected in a characteristic stretching of the global mobility function ($\ln F(t) \sim -\sqrt{t}$) and the autocorrelation function $C(t) \sim 1/\sqrt{t}$). This crossover can be observed also for very short times, because the distribution of blocked chains determines of course the coefficients Γ_k and therefore also the relaxation behavior of the analyzed quantities.

Another important result is the strong difference between $F(t)$ and $C(t)$. Numerical simulations[18] (for a SFM[2, 2]) at moderate temperatures suggest an approximately equivalence $F(t) \sim C(t)$. But the analytical results show that at least for sufficiently low temperatures both quantities are strongly different.

Furthermore, the model supports the picture of an increasing dynamical heterogeneity[30, 31] with decreasing temperature, i.e., the kinetic motion is restricted to the neighbors of mobile cell (a cell in the state $\sigma = 1$). All other cells, especially the cells in the long blocked chains are completely frozen.

At the end let us make a short remark to the above applied techniques. Both, mean field approximation (Section III.A.1) and series expansion leads to practicable results, even if the accuracy is not to strong. Slightly better results can be obtained for short times from the solution of the infinite hierarchical system of evolution equations[19] and for long times from the above discussed kinetic approach. Both techniques allow a complete prediction of the numerical simulations.

APPENDIX A. PARTIAL SUMMATION

A possible approach to the infinite series (15) can be obtained by using reasonable approximations of the Γ_k for sufficiently large k. To this aim it is necessary to find an answer to the following three questions:

1. How many n-point diagrams exist at a given order k (the operator $\hat{L}$ had been applied k-times)?

2. Which fraction of these diagrams has only one open circle localized at the initial position?

3. What are the prefactor of those diagrams?

To answer the first question let us introduce the number of diagrams R^k which are created after k steps. R^k can be decomposed into different fractions R_n^k which contains the diagrams with n points ($n \leqslant k+1$):

$$R^k = \sum_{n=0}^{k+1} R_n^k$$

Inspecting the diagrammatic rules we get the following recursion relation

$$R_{n+1}^{k+1} = R_{n+1}^k[2(n-1)+2] + 2R_n^k = 2(nR_{n+1}^k + R_n^k) \tag{A1}$$

The first term contains all diagrams which does not change the number of points by an application of $\hat{L}$, whereas the second term includes all diagrams which contains a new point created by a subsequent application of $\hat{L}$. Taking into account the initial and boundary conditions $R_n^0 = \delta_{n1}$, $R_1^k = \delta_{k0}$ and $R_0^k \equiv 0$ one obtains the rigorous solution of (A1)

$$R_n^k = \sum_{\mu}^{n-1} (-1)^{n-1-\mu} \frac{(2\mu)^k}{(n-1-\mu)!\,(\mu)!} \tag{A2}$$

Obviously not all R_n^k graphs will contribute to Γ^k.

An approximate answer to the second question can be obtained by mean-field arguments. For that we analyze a diagram with n points at the order k. The application of $\hat{L}$ leads either to an extension of the graph by an additional point or to a change of the sequence of bullets and circles along the chain. The frequency to find a graph of order k and n points with m circles (and $n-m$ bullets) is given by the probability distribution $\omega_n(m, k)$. The determination of $\omega_n(m, k)$ bases initially on a subclass of diagrams, which are formed firstly by $n-1$ growing steps whereas further steps changes only the sequence of bullets and circles (i.e., the length of the graph is conserved). We make the assumption that this subclass is a representative one of all other graphs of order k with n points (this can be legitimeted by inspecting directly the diagrams with relative small n). We study the change of the sequence in the framework of a mean field theory. Under consideration that the previous sequence (order k) has m circles, the following changes are possible (see also Fig. 11):

1. Application of $\hat{L}$ (or more precisely $\hat{l}$) on a circle (the circle is conserved by this application, see below): If simultaneously the neighbor affected by this procedure is also a circle then it will be transformed into

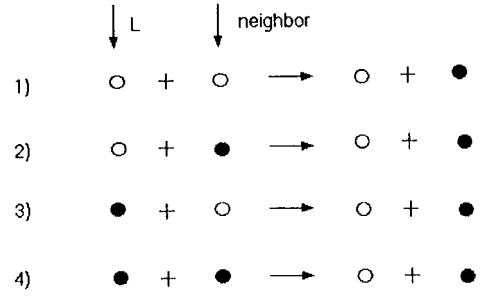

Fig. 11. Schematic "reactions" inside a diagram. In terms of the mean field theory there is no correlation to the actual spatial distribution of the bullets and items. The arrows indicate the application of L and the simultaneously affected neighbor, respectively.

a bullet, i.e., the new sequence loses a circle and wins an additional bullet. The relative frequency for the existence of neighbored circles is given by $m(m-1)/n(n-1)$.

2. Application of $\hat{L}$ on a circle: If the neighbor affected simultaneously is now a bullet, the sequence will not be changed. The frequency that a circle and a bullet are in the neighborhood is given by $m(n-m)/n(n-1)$.

3. Application of $\hat{L}$ on a bullet which will be transformed into a circle: If the affected neighbor is a circle, this point becomes after the application of $\hat{L}$ a bullet. Thus, the number of circles and bullets of the total graph is conserved, only the position is changed. The frequency for this process is also $m(n-m)/n(n-1)$.

4. Application of $\hat{L}$ on a bullet: If the affected neighbor is also a bullet the number of circles increases and consequently one bullet disappears. The frequency is $(n-m)(n-m-1)/n(n-1)$.

Thus in mean field approximation we find the discrete Chapman–Kolmogorov equation:

$$\omega_n(m, k+1) = \frac{m(m+1)}{n(n-1)}\omega_n(m+1, k) + 2\frac{m(n-m)}{n(n-1)}\omega_n(m, k) + \frac{(n-m)(n+1-m)}{n(n-1)}\omega_n(m-1, k) \tag{A3}$$

The stationary solution $\omega_0(m)$ of (A3) fulfils the self consistent relation $\omega(m, k) = \omega(m, k+1)$. Hence $\omega_0(m)$ is given by the normalized solution

$$\omega_0(m) = \frac{\Gamma(n+1)\,\Gamma(n-1)}{\Gamma(2n-1)}\binom{n-1}{m}\binom{n-1}{m-1}$$

The stationary solution is the rigorous solution of (A3) for $k \to \infty$. For the following investigation we assume that the rigorous solution of the (A3) can be approximated by the stationary solution for $k \geqslant 2n$. The fraction of diagrams with exact one circle is given by

$$\omega_0(1) = \frac{\Gamma(n+1)\,\Gamma(n)}{\Gamma(2n-1)}$$

and the fraction of diagrams with only one circle at the original position (corresponding to the initial cell (i) becomes

$$\tilde{\omega}_n = \frac{\omega_0(1)}{n} = \frac{\Gamma^2(n)}{\Gamma(2n-1)} \tag{A4}$$

Furthermore it is a simple consideration that a diagram with n points but only one circle exists only if the order k is restricted by $k \geqslant 2n-4$ ($n \geqslant 2$). Therefore, the total number of relevant graphs of order k with n points is given by

$$Z_n^k = R_n^k \tilde{\omega}_n \Theta(k+4-n)$$

$\Theta(x)$ is the usual step function ($\Theta(x \geqslant 0) = 1$ and $\Theta(x < 0) = 0$).

The last question concerns the determination of an averaged prefactor of these graphs. Here we consider only the of low temperature regime, i.e., $\bar{\sigma}_{\text{eq}} \to \infty$. The extension to higher temperatures is always possible. The formation of a diagram with only one circle (all other points are bullets) from one initial circle would indicate that the number of created and annihilated circles must be equivalent. Thus the number of prefactors $\sqrt{\bar{\sigma}_{\text{eq}}(1-\bar{\sigma}_{\text{eq}})}$ and $\sqrt{(1-\bar{\sigma}_{\text{eq}})/\bar{\sigma}_{\text{eq}}}$ is also equivalent, i.e., the total prefactor power of $1-\bar{\sigma}_{\text{eq}} \approx 1$ and can be neglected. On the other hand, each final bullet produces a factor $\bar{\sigma}_{\text{eq}}$. Thus a diagram with n points has the weight $\bar{\sigma}_{\text{eq}}^{n-1}$.

Finally, one obtains

$$\Gamma_k = \sum_{n=1}^{\infty} Z_n^k \bar{\sigma}_{\text{eq}}^{n-1} = \sum_{n=1}^{\infty} R_n^k \tilde{\omega}_n \Theta(k+4-n)\, \bar{\sigma}_{\text{eq}}^{n-1}$$

Using (15), (A2) and (A4) we end up with the final expression for the correlation function

$$C(t) = \sum_{n=1}^{\infty} \bar{\sigma}_{\text{eq}}^{n-1} \frac{\Gamma^2(n)}{\Gamma(2n-1)} \sum_{\mu}^{n-1} \frac{(-1)^{n-1-\mu}}{(n-1-\mu)!\,(\mu)!} \sum_{k=0}^{\infty} \frac{(2\mu)^k}{k!} \left(-\frac{t}{\tau_0}\right)^k \tag{A5}$$

REFERENCES

1. W. Götze in *Liquids, Freezing and the Glass Transition*, Hansen *et al*., eds. (North Holland, Amsterdam, 1991).
2. W. Götze and L. Sjögren, *Rep. Prog. Phys.* **55**:241 (1992).
3. J. Jäckle, *Rep. Prog. Phys.* **49**:171 (1986).
4. E. Leutheusser, *Phys. Rev. A* **29**:2765 (1984).
5. G. Adams and J. H. Gibbs, *J. Chem. Phys.* **43**:139 (1965).
6. M. L. Williams, R. F. Landel, and J. D. Ferry, *J. Am. Chem. Soc.* **77**:3701 (1955).
7. W. Götze and L. Sjögren, *Zeitschrift für Physik B Cond. Matter* **65**:415 (1987).
8. W. Götze and L. Sjögren, *J. Phys. C* **21**:3407 (1988).
9. T. Franosch, W. Götze, M. R. Mayr, and A. P. Singh, *Phys. Rev. E* **55**:3183 (1997).
10. T. Franosch, M. Fuchs, W. Götze, M. R. Mayr, and A. P. Singh, *Phys. Rev. E* **55**:7153 (1997).
11. G. H. Fredrickson and H. C. Andersen, *J. Chem. Phys.* **84**:5822 (1985).
12. G. H. Fredrickson and H. C. Andersen, *Phys. Rev. Lett.* **53**:1244 (1984).
13. G. H. Fredrickson, *Ann. Rev. Phys. Chem.* **39**:149 (1988).
14. G. H. Fredrickson and S. A. Brawer, *J. Chem. Phys.* **84**:3351 (1986).
15. M. Schulz and P. Reinecker, *Phys. Rev. B* **48**:9369 (1993).
16. M. Schulz and P. Reinecker, *Phys. Rev. B* **52**:4131 (1995).
17. M. Schulz, P. R. S. Sharma, and H. L. Frisch, *Phys. Rev. B* **52**:7195 (1995).
18. S. Butler and P. Harrowell, *J. Chem. Phys.* **95**:4454 (1991).
19. M. Schulz and S. Trimper, *Int. J. Mod. Phys. B* **11**:2927 (1997).
20. J. Doi, *Phys. A: Math. Gen.* **9**:1465 (1976).
21. S. Sandow and S. Trimper, *Europhys. Lett.* **21**:799 (1993).
22. P. Grassberger and M. Scheunert, *Fortschr. Physik* **28**:547 (1980).
23. L. Peliti, *J. Physique* **46**:1469 (1985).
24. G. Schütz and S. Sandow, *Phys. Rev. E* **49**:2726 (1994).
25. L. H. Gwa and H. Spohn, *Phys. Rev. Lett.* **68**:725 (1992).
26. F. C. Alcarez, M. Droz, M. Henkel, and V. Rittenberg, *Ann. Phys. (N.Y.)* **230**:250 (1994).
27. M. Schulz and S. Trimper, *Phys. Lett. A* **216**:235 (1996).
28. N. G. van Kampen, *Stochastic Processes in Physics and Chemistry* (North-Holland, Amsterdam, 1986).
29. C. W. Gardiner, *Handbook of Stochastic methods* (Springer-Verlag, Berlin, 1983).
30. R. Richert, *Chem. Phys. Lett.* **216**:223 (1993).
31. R. Böhmer, G. Hinze, G. Diezemann, B. Geil, and H. Sillescu, *Europhys. Lett.* **36**:55 (1996).